IEEE Photonics Journal
An IEEE Photonics Society Publication

Open Access

Generation of One-Dimensional Terahertz Airy Beam by Three-Dimensional Printed Cubic-Phase Plate

Volume 9, Number 4, August 2017

Liting Niu
Changming Liu
Qiao Wu
Kejia Wang
Zhengang Yang
Jinsong Liu

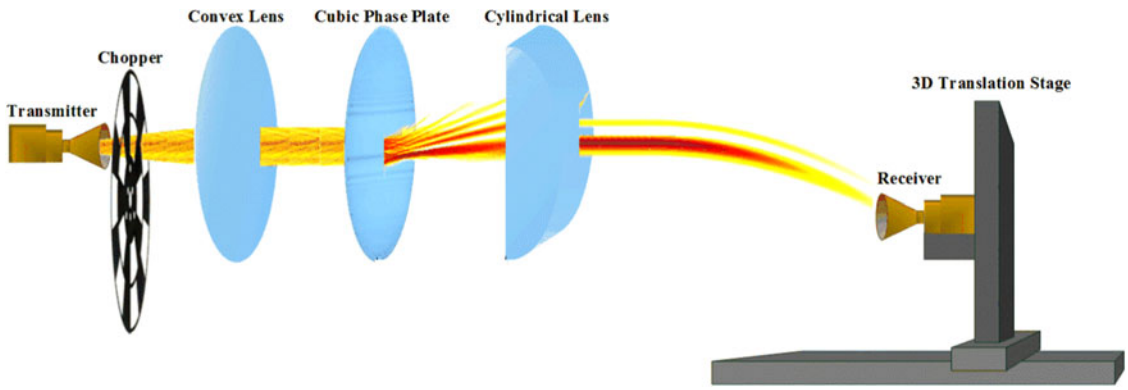

DOI: 10.1109/JPHOT.2017.2712615
1943-0655 © 2017 IEEE

IEEE photonics SOCIETY

IEEE

Generation of One-Dimensional Terahertz Airy Beam by Three-Dimensional Printed Cubic-Phase Plate

Liting Niu, Changming Liu, Qiao Wu, Kejia Wang, Zhengang Yang, and Jinsong Liu

Wuhan National Laboratory for Optoelectronics, Huazhong University of Science and Technology, Wuhan 430074, China

DOI:10.1109/JPHOT.2017.2712615

Manuscript received April 25, 2017; revised May 29, 2017; accepted June 1, 2017. Date of publication June 7, 2017; date of current version June 28, 2017. This work was supported by the National Natural Science Foundation of China under Grants 11574105 and 61177095. Corresponding author: Jinsong Liu (e-mail: jsliu4508@vip.sina.com).

Abstract: We first present the one-dimensional (1-D) terahertz (THz) Airy beam with a 0.3-THz continuous wave. The required phase modulation and the optical Fourier transform are implemented with a 3-D printed cubic-phase plate (CPP) and a cylindrical lens, respectively. According to the parameter of the designed CPP, we numerically calculate the intensity distributions of the 1-D THz Airy beam in the free space. The experimental results show a good accordance with the theoretical ones. Additionally, by blocking part of the generated 1-D Airy beam with a metal screen, the beam exhibits a self-healing property, i.e., tends to reform during propagation.

Index Terms: Airy beam, terahertz, three-dimensional printing.

1. Introduction

In 1979, Berry and Balazs proposed that the SchrÖdingr equation describing the wave packet of a free particle exists in the form of the Airy function [1]. Particularly, they pointed out that the Airy wave packet solution is the only shape-preserving accelerating solution to the SchrÖdingr equation in $(1 + 1)$D configurations [1], [2]. In the comparison of the SchrÖdingr equation and the paraxial equation of diffraction, one can find out that the Airy wave packet can also be a solution of the paraxial equation of diffraction [3]. Hence in 2007, Siviloglou *et al.* numerically investigated the optical Airy beam and proposed the method that generated finite power Airy beam by considering its exponentially decaying version. Even though in this case, the truncated Airy beam can still preserve its shape over several diffraction lengths and self-bending in the transverse direction [4], [5].

Subsequently the self-healing property of the truncated Airy beam was studied and the result showed that it tended to reform during propagation even in the case of severe perturbation [6].

In recent years, various applications based on the Airy beam are developed because of its peculiar properties. Such as light bullet [7], [8], optical routing [9], micro particles manipulating [10]–[12] and light-sheet microscopy [13], [14]. Moreover, referring to the principle of optical Airy beams, the Airy function can also be utilized in the acoustic [15] and plasma fields [16], [17]. However, most of

these applications are concentrated in the optical domain, to the best of our knowledge, there are no research of the 1D Airy beam in the THz domain.

Owning to Siviloglou's great work, the finite Airy beam was first obtained by a system that consists of a spatial light modulator (SLM) and a Fourier transform lens. The SLM was used to impose the cubic phase to Gaussian beam and the Fourier transform lens was used to perform Fourier transform [4]. One of the drawbacks of this system is its length, because the focal length of the Fourier transform lens is 1.2 m [5], which is extremely long for most laboratories. Therefore, Davis *et al.* proposed the method that incorporating the Fresnel diffraction and the Fourier transform lens onto a liquid crystal display (LCD) to reduce the system length [18], [19]. Subsequently, more compact systems, such as Airy beam lasers were put forward [20], [21]. The power conversion efficiency of all the systems mentioned above is low, for example, the efficiency of the system involves LCD is less than 40% because of the damage threshold of the LCD [22], [23]. In addition, they have other practical limitations, for example, the modulators are expensive and the special nonlinear optical materials are difficult to achieve. Yuan *et al.* proposed a high efficiency approach that generated Airy beam with a micro-fabricated cubic phase plate (CPP) which had high damage threshold [22]. However, this method is not applicable to THz domain because the materials with the desired terahertz modulation are lacking. Fortunately, inspired by our previous work, we believe that the 3D printing technology is feasible to be used to produce the 1D THz Airy beam [23]–[25].

In this paper, we generate the 1D THz Airy beam with a 0.3-THz continuous wave. A 1D CPP is designed and fabricated with a commercial 3D printer, which is incorporated with a cylindrical lens to produce the 1D THz Airy beam. Besides, a metal screen is used to block part of the beam for investigating the self-healing property of the 1D THz Airy beam. The results show that the 1D THz Airy beam remains almost invariant up to a distance of 100 mm while it tends to self-bending, and the disturbed 1D Airy beam tends to reform even the perturbation is severe. The generated 1D THz Airy beam exhibits non-diffracting and self-healing properties which could benefit the applications of focal depth extended THz imaging systems and robust THz wireless communication links, respectively.

2. Concept and Fabrication of the Cubic Phase Plate

It is well-known that the ideal Airy beam is impossible in the experimental environment because of its infinite energy. A feasible way to realize the finite energy Airy beam is introducing an exponential truncation function, i.e. the initial plane of Airy beam is set as $\phi(s, 0) = \mathrm{Ai}(s)\exp(\alpha s)$. Here $s = x/x_0$ is the dimensionless transverse coordinate, x is the transverse coordinate, x_0 is an arbitrary transverse scale, and α is the exponential truncation factor [4]. It should be noted that α is a positive parameter and it is much less than 1 so that the truncated Airy beam still presents all the properties of the ideal Airy beam. Under the above conditions, the propagation dynamics of the finite energy Airy beam is as follows:

$$\phi(s, \xi) = Ai\left(s - \left(\frac{\xi}{2}\right)^2 + i\alpha\xi\right)\exp\left(\alpha s - \frac{\alpha\xi^2}{2} - \frac{i\xi^3}{12} + i\alpha^2\frac{\xi}{2} + is\frac{\xi}{2}\right) \tag{1}$$

Here $\xi = z/k_0x_0^2$ is a normalized propagation distance, z is the longitudinal coordinate and k_0 is the wave number of the optical wave [4], [5]. The propagation dynamics of the finite energy Airy beam in the xz-plane can be obtained theoretically according to this equation.

As proposed by Siviloglou *et al.* the Fourier spectrum $\Phi(k)$ of the wave packet $\phi(s, 0)$ in the normalized k-space is proportional to $\exp(-\alpha k^2)\exp(ik^3/3)$. Here k is the coordinate of the spectral space [3], [4]. Obviously, the angular Fourier spectrum of the infinite energy Airy beam is a Gaussian beam that involves a cubic phase front. Here, we intend to generate 1D THz Airy beam with a 0.3-THz continuous wave. The required cubic phase is in the form of

$$\Psi_x = \beta x^3 \tag{2}$$

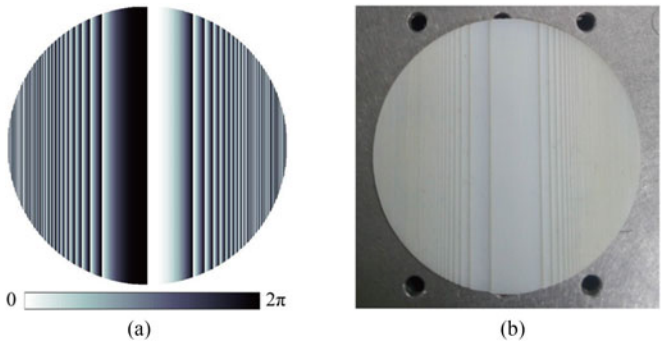

Fig. 1. (a) The phase profile of the 1D CPP, which is wrapped between $[0, 2\pi]$. 0 and 2π correspond to black and white respectively. (b) The optical photograph of the 1D CPP. The thickness of this CPP varies between 2 mm and 3.5 mm.

Here β is the scaling factor of the cubic phase and x is the transverse coordinate. Clearly, the Gaussian beam carrying the cubic phase is proportional to $\exp(-x^2/\omega_0^2)\exp(i\beta x^3)$, where ω_0 is the waist radius of the Gaussian beam. By comparing the expressions $\exp(-x^2/\omega_0^2)\exp(i\beta x^3)$ and $\exp(-\alpha k^2)\exp(ik^3/3)$, it is can be deduced that

$$\alpha = \omega_0^{-2}(3\beta)^{-\frac{2}{3}} \tag{3}$$

According to (2), the cubic phase changes in the range of -691 to 691 radians on the condition that the scaling factor β is 0.0125 and transverse coordinate is within the range from -38.1 mm to 38.1 mm.

It is well known that a beam propagates a distance of h in a uniform medium in the free space the phase shift of the beam can be calculated as $2\pi(n-1)h/\lambda$, where λ is the wavelength of the beam and n is the refractive index of the medium. Hence, a 1D CPP with varying thickness can be produced according to the equivalency between phase shift and optical path for imprinting the cubic phase into the incident beam. In our experiments, the 1D CPP is fabricated by Object30 3D printer and the printing material is Full Cure 835 Vero White. The refractive index n and the absorption coefficient of the material is 1.655 and 1.5 cm^{-1} respectively, which are characterized by a Zomega-Z3 THz Time-Domain Spectroscopy. As the maximum phase shift is 1382 radians, which is the variation range of the cubic phase, the maximum thickness of the CPP is calculated to be 336 mm. Obviously, The CPP is so thick that it is hard to fabricate and not suitable for the experiment setup. Moreover, the absorption loss of the THz wave cannot be overlooked. To solve these problem, the phase profile is wrapped between $[0, 2\pi]$. As shown in Fig. 1(a), 0 and 2π correspond to black and white respectively. In this instance, the thickness of the 1D CPP varies between 0 and 1.5 mm. However, the CPP will be divided into small pieces because of containing many zero thickness. For this reason, the CPP should be added a base. The thickness of the CPP is given by

$$h(x, y) = \frac{\lambda}{2\pi(n-1)}\text{rem}_{2\pi}[\Psi_x - \min(\Psi_x)] + h_0 \tag{4}$$

Here $\min(\Psi_x)$ is the function to obtain the minimum value of Ψ_x and the value is -691 radians, rem is a function of remainder to ensure the phase profile be wrapped in the range of $[0, 2\pi]$, h_0 is the base thickness of the CPP. In the condition of $h_0 = 2$ mm, the maximun thickness of the CPP is calculated to be 3.5 mm. The CPP fabricated by Object30 3D printer is shown in Fig. 1(b). Fortunately, the surface of the CPP is smooth because the Object30 3D printer has a resolution of 600 dpi (42 μm) in the x and y directions and 900 dpi (28 μm) in the z direction.

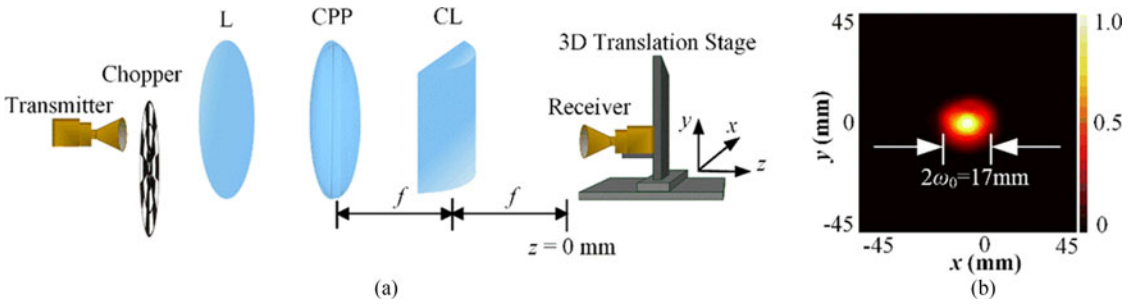

Fig. 2. (a) Schematic of experimental setup for generating and measuring the 1D THz Airy beam. L: Lens. CPP: cubic phase plate. CL: cylindrical lens. (b) The normalized intensity distribution of the collimated beam that is incident upon the CPP.

3. Experimental Setup and Results

The experimental setup is schematically shown in Fig. 2(a). The transmitter is composed of a 0.1-THz Gunn diode (Spacek Labs Inc., GW-102P), a frequency tripler (Virginia Diode Inc., WR-3.4) and a horn antenna (Virginia Diode Inc., WR-3.4CH). The Gunn diode is coupled with the frequency tripler to deliver 0.3-THz continuous wave, whose output power is 0.3 mW. The horn antenna is used to emit the THz wave into the free space. The THz beam is collimated by a high-density polyethylene (HDPE) convex lens and then is directed onto the CPP to impose the cubic phase modulation. The direction of the thickness change is parallel to the x direction. A HDPE cylindrical lens (the focal length f = 100 mm) is placed behind the CPP with a distance of focal length to obtain the Fourier transform of the phase-modulated Gaussian beam and the direction of the focal line is parallel to the x direction. Detection is implemented by a receiver that consists of a Schottky diode (Virginia Diode Inc., WR-3.4ZBD) and a horn antenna. The THz beam is modulated at 400 Hz by a mechanical chopper and the output signal of the THz detector is fed into a lock-in amplifier. With the use of the chopper and the lock-in amplifier, the 1D THz Airy beam generation system has the merits of large dynamic range and high signal-to-noise ratio (SNR). To investigate the propagation of the 1D THz Airy beam, we mount the receiver on a three-axes motorized translation stage and choose a raster scanning method. The detection area in the xz-plane (y = 0 mm) is 90 mm × 300 mm and the pixel number is 181 × 301, while the detection area in the xy-plane is 90 mm × 90 mm and the pixel number is 181 × 91.

The normalized intensity distribution of the collimated beam that incidents to the CPP is shown in Fig. 2(b). In the color scale pattern, black and white correspond to 0 and 1.0 respectively. As shown in the figure, the width of the collimated beam is $2\omega_0 = 17$ mm, where ω_0 is the waist radius of the Gaussian beam.

Theoretical calculation for the propagation of the 1D THz Airy beam in the xz-plane is obtained according to the (1). The exponential truncation factor α in the equation is 0.1235, which is determined by the scaling factor $\beta = 0.0125$ and the waist radius $\omega_0 = 8.5$ mm. The simulation area is 90 mm × 300 mm in the xz-plane corresponding to y = 0 mm, which is consistent with the detection area of the experiment. The corresponding calculation result is shown in Fig. 3(a). As we can see, the main lobe of the generated 1D THz Airy beam almost keeps its shape over a distance of 100 mm, which indicates the non-diffracting feature of the 1D THz Airy beam. More importantly, the Airy beam exhibits a self-bending characteristic during propagation in the free space.

The beam demonstrated in Fig. 3(b) is generated by the experimental setup described above and detected in the xz-plane (y = 0 mm). It should be noted that this beam preserves the non-diffracting and self-bending properties in the propagation, which is consistent with the ones demonstrated in Fig. 3(a). Compared with Fig. 3(a), it is clear that the main lobe of the Airy beam on the initial plane in Fig. 3(b) is located at the same position and has the same full width at half maximum (FWHM). However, the side lobes are less and the intensity attenuates faster, perhaps because of the low power of the THz transmitter and the attenuation of the beam in the propagation.

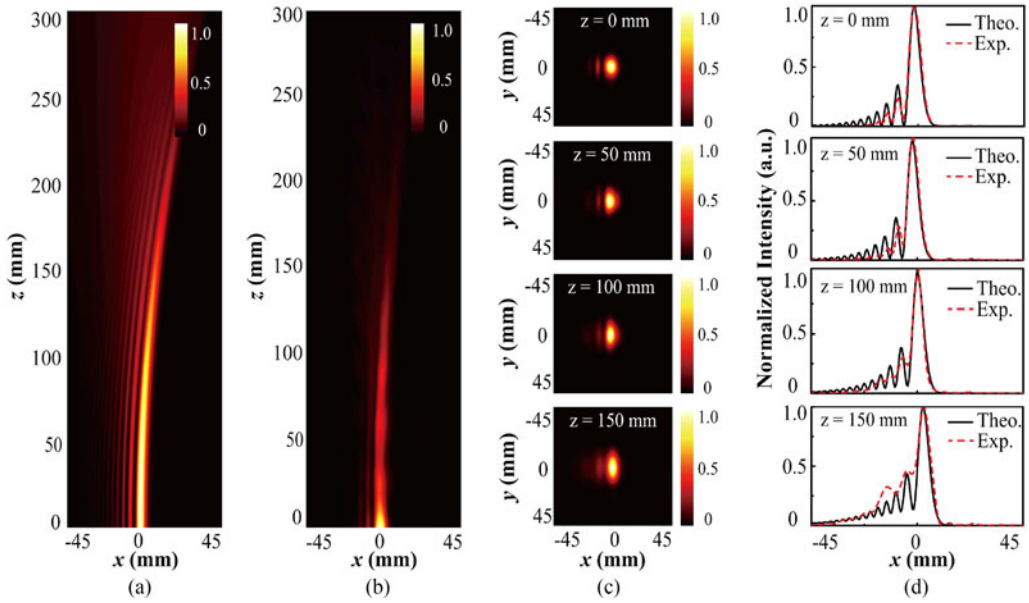

Fig. 3. The 1D THz Airy beam: (a) Theoretical calculation for the propagation of the beam in the xz-plane. (b) Propagation of the beam generated experimentally in the xz-plane. (c) The transverse intensity distributions in the xy-plane at various distances. (d) Comparison of the normalized intensity profiles between theory and experiment at various distances. The black solid lines and the red dash lines correspond to the theoretical intensity profiles and the experimental ones.

For further investigation, the transverse intensity distribution of the 1D THz Airy beam at various distances are shown in Fig. 3(c). Obviously, the main lobe of the Airy beam is almost invariant while it is transverse accelerating in the x direction, which is in line with the propagation of the beam in Fig. 3(b). It is to be noted that the main lobe of the beam is spreading in the y direction, which may be caused by the mismatch of the elements in the experimental setup. The experimental result demonstrated that the intensity profiles of the 1D THz Airy beam is Airy function in the x direction and it is Gaussian function in the y direction, which is because the cubic phase modulation and the optical Fourier transform of the Gaussian beam only exist in the x direction.

Fig. 3(d) demonstrated the detail comparison of the 1D THz Airy beam generated by theory and experiment at various propagation distances. The black solid lines and the red dash lines in the figures are corresponding to the theoretical intensity profiles and the experimental ones, respectively. It is demonstrated that the 1D THz Airy beam obtained theoretically and experimentally both keep their shapes unaltered and are self-bending in the propagation. The main lobe of the 1D THz Airy beam obtained experimentally is in good agreement with the theoretical one, but the side lobes correspond to the experiment are not according with the theoretical ones, which are possibly caused by the small transmitter power and the absorption. Besides, the components in the experimental setup do not align perfectly may be part of the reason.

To investigate the self-healing property of the 1D THz Airy beam, a rectangular metal screen with an area of 99 mm $\times$ 101 mm and a thickness of 0.25 mm is placed in the back focal plane of the cylindrical lens (z $=$ 0 mm) to prevent the transmission of THz wave located in the area where the transverse coordinate x is smaller than -5 mm. All side lobes and part of the main lobe of the 1D THz Airy beam are obstructed at the origin plane. Experimental results of the disturbed 1D THz Airy beam propagation in free-space are presented in Fig. 4, where Fig. 4(a) shows the propagation dynamics of the disturbed Airy beam in the xz-plane (y $=$ 0 mm). Fig. 4(b) and (c) indicates the transverse intensity distributions of this beam in the xy-plane and the normalized intensities of the beam in the x direction, respectively. They are detected in the propagation distances of z $=$ 0 mm, z $=$ 50 mm, z $=$ 100 mm and z $=$ 150 mm. We note that all of the side lobes and part of the main

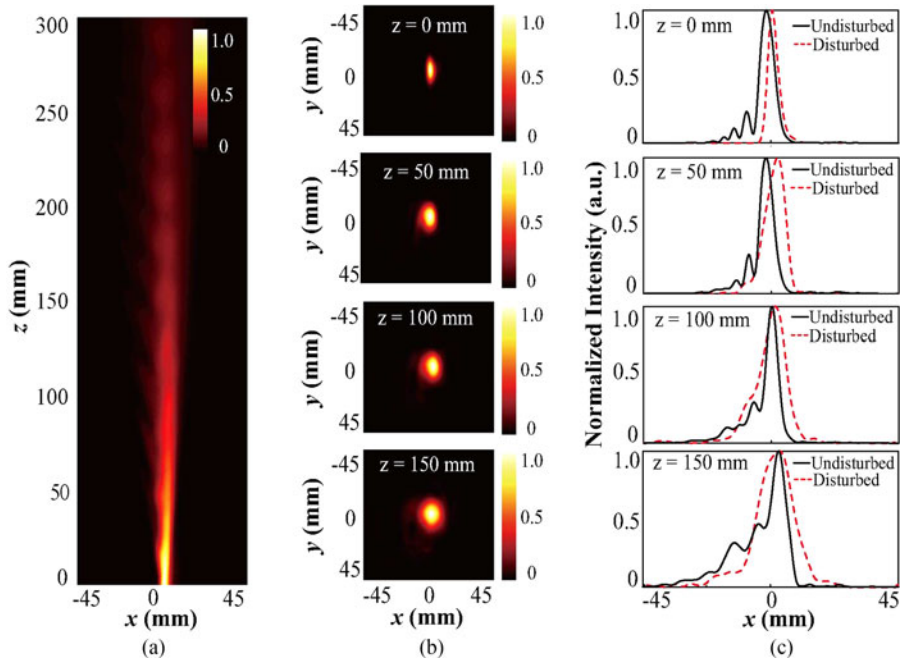

Fig. 4. The self-healing property of 1D THz Airy beam: (a) the propagation of the partially blocked Airy beam observed in the xz-plane, (b) The transverse intensity distributions in the xy-plane at the distance of z = 0 mm, z = 50 mm, z = 100 mm, z = 150 mm. (c) The normalized intensity comparison of the disturbed 1D THz Airy beam and the undisturbed one in the x direction at z = 0 mm, z = 50 mm, z = 100 mm, z = 150 mm. The black solid lines and the red dash lines correspond to the undisturbed 1D THz Airy beam and the disturbed ones.

lobe of the 1D THz Airy beam are blocked in the origin plane, which is more obvious in the first rows of Fig. 4(b) and (c). The second and third rows of Fig. 4(c) shows the main lobe has partly reformed at z = 50 mm. Besides, the main lobe remains almost invariant from the propagation distance of z = 50 mm to z = 100 mm while it tends to self-bending. However, the side lobes are not recovered during propagation perhaps because the interruption is severe and the remaining energy is too little.

4. Conclusion

In summary, we both theoretically and experimentally demonstrate the 1D Airy beam with a 0.3-THz continuous wave. Our investigation confirms that the 1D THz Airy beam can be generated with a 1D CPP and a cylindrical lens. It is conceived that other optical components used in THz domain can be manufactured by 3D printing technology. The 1D THz Airy beam can be applied to THz imaging techniques such as THz computed tomography, time-of-flight terahertz tomography, and tomosynthesis. In our future work, the THz Airy beam will be used in these THz imaging systems to improve image quality.

References

[1] C. W. Wong, "Nonspreading wave packets," *Amer. J. Phys.*, vol. 47, no. 3, pp. 264–267, 1979.
[2] K. Unnikrishnan and A. R. P. Rau, "Uniqueness of the Airy packet in quantum mechanics," *Amer. J. Phys.*, vol. 64, no. 8, pp. 1034–1035, 1996.
[3] F. M. Fernández, "Algebraic approach to non-spreading wavepackets," *Eur. J. Phys.*, vol. 18, no. 6, pp. 440–443, 1997.
[4] G. A. Siviloglou and D. N. Christodoulides, "Accelerating finite energy Airy beams," *Opt. Lett.*, vol. 32, no. 8, pp. 979–981, 2007.

[5] G. A. Siviloglou, J. Broky, A. Dogariu, and D. N. Christodoulides, "Observation of accelerating Airy beams," *Phys. Rev. Lett.*, vol. 99, no. 21, 2007, Art no. 213901.
[6] J. Broky, G. A. Siviloglou, A. Dogariu, and D. N. Christodoulides, "Self-healing properties of optical Airy beams," *Opt. Exp.*, vol. 16, no. 17, pp. 12880–12891, 2008.
[7] D. Abdollahpour, S. Suntsov, D. G. Papazoglou, and S. Tzortzakis, "Spatiotemporal Airy light bullets in the linear and nonlinear regimes," *Phys. Rev. Lett.*, vol. 105, no. 25, 2010, Art. no. 253901.
[8] A. Chong, W. H. Renninger, D. N. Christodoulides, and F. W. Wise, "Airy-Bessel wave packets as versatile linear light bullets," *Nature Photon.*, vol. 4, no. 2, pp. 103–106, 2010.
[9] P. Rose, F. Diebel, M. Boguslawski, and C. Denz, "Airy beam induced optical routing," *Appl. Phys. Lett.*, vol. 102, no. 10, pp. 101101–101101-3, 2013.
[10] J. Baumgartl, M. Mazilu, and K. Dholakia, "Optically mediated particle clearing using Airy wavepackets," *Nature Photon.*, vol. 2, no. 11, pp. 675–678, 2008.
[11] J. Baumgartl, G. M. Hannappel, D. J. Stevenson, D. Day, M. Gu, and K. Dholakia, "Optical redistribution of microparticles and cells between microwells," *Lab Chip*, vol. 9, no. 10, pp. 1334–1336, 2009.
[12] J. Baumgartl *et al.*, "Optical path clearing and enhanced transmission through colloidal suspensions," *Opt. Exp.*, vol. 18, no. 16, pp. 17130–17140, 2010.
[13] S. Jia, "Super-resolution imaging with Airy beams," presented at the Frontiers in Optics Meeting, San Jose, CA, USA, Oct. 18–22, 2015.
[14] T. Vettenburg *et al.*, "Light-sheet microscopy using an Airy beam," *Nature Methods*, vol. 11, no. 5, pp. 541–544, 2014.
[15] A. Arie, B. K. Singh, R. Remez, and Y. Tsur, "Super-Airy beam: self-accelerating beam with intensified with intensified main lobe," *Opt. Lett.*, vol. 40, no. 20, pp. 4703, 2015.
[16] P. Polynkin, M. Kolesik, J. Moloney, G. Siviloglou, and D. Christodoulides, "Curved plasma channel generation in air using ultra-intense self-bending Airy beams," *Opt. Photon. News*, vol. 20, no. 12, p. 28, 2009.
[17] P. Polynkin, M. Kolesik, and J. Moloney, "Filamentation of femtosecond laser Airy beams in water," *Phys. Rev. Lett.*, vol. 103, no. 12, 2009, Art. no. 123902.
[18] J. A. Davis, D. M. Cottrell, and J. M. Zinn, "Direct generation of abruptly focusing vortex beams using a 3/2 radial phase-only pattern," *Appl. Opt.*, vol. 52, no. 9, pp. 1888–1891, 2013.
[19] J. A. Davis, M. J. Mitry, M. A. Bandres, I. Ruiz, K. P. Mcauley, and D. M. Cottrell, "Generation of accelerating Airy and accelerating parabolic beams using phase-only patterns," *Appl. Opt.*, vol. 48, no. 17, pp. 3170–3176, 2009.
[20] S. Longhi, "Airy beams from a microchip laser," *Opt. Lett.*, vol. 36, no. 5, pp. 716–718, 2011.
[21] G. Porat, I. Dolev, O. Barlev, and A. Arie, "Airy beam laser," *Opt. Lett.*, vol. 36, no. 20, pp. 4119–4121, 2011.
[22] R. Cao, Y. Yang, J. Wang, J. Bu, M. Wang, and X. C. Yuan, "Microfabricated continuous cubic phase plate induced Airy beams for optical manipulation with high power efficiency," *Appl. Phys. Lett.*, vol. 99, no. 26, 2011, Art. no. 213901.
[23] C. Liu, L. Niu, K. Wang, and J. Liu, "3D-printed diffractive elements induced accelerating terahertz Airy beam," *Opt. Exp.*, vol. 24, no. 25, pp. 29342–29348, 2016.
[24] X. Wei *et al.*, "Generation of arbitrary order Bessel beams via 3D printed axicons at the terahertz frequency range," *Appl. Opt.*, vol. 54, no. 36, pp. 10641–10649, 2015.
[25] C. Liu, X. Wei, L. Niu, K. Wang, Z. Yang, and J. Liu, "Discrimination of orbital angular momentum modes of the terahertz vortex beam via diffractive elements," presented at CLEO: Applications Technology, 2016, Paper JTh2A.62.